Unconventional domain bands near a crack tip

W. Yang, F. Fang, H.T. Wang and Y.Q. Cui
Department of Engineering Mechanics, Tsinghua University,
Beijing 100084, P.R. China
Tel. 86-10-62782642, Fax: 86-10-62781824, e-mail: yw-dem@tsinghua.edu.cn

Abstract

Experiment indicates that unconventional domain band structure appears ahead of an indentation crack tip, and it is caused by the highly localized crack tip electric field. The partially switched ferroelectric grain resembles a banded Eshelby inclusion embedded in a polycrystalline ferroelectric matrix. Mesomechanics analysis quantifies the unconventional domain band structures, including the volume fraction, the thickness, and the orientation of switched domain bands. The interaction between cracking and domain switching in single crystal ferroelectrics is also discussed.

1. Introduction

Ferroelectric ceramics exhibit peculiar behaviors such as fracture near a defect or an electrode under electric load [1]. The intensive electric field near a crack tip stimulates local domain polarization switching that plays a critical role in electric fracture. The switched domains generate incompatible strain under the constraint of un-switched material and consequently alter the stress distribution near the crack. Experiment [2] indicates that unconventional domain band structure appears ahead of an indentation crack tip when subjected to lateral electric field. The band structure is caused by highly localized crack tip electric field. The elastic mismatch energy for a partially switched ferroelectric grain embedded in a polycrystalline ferroelectric matrix is evaluated as a banded Eshelby inclusion. The discussion is extended to the interaction between cracking and domain switching in single crystal ferroelectrics.

2. Microscopy of Crack Tip Unconventional Domain Bands

Experimental observations for domain bands were mostly reported under uniform fields. It was the work in [2] that provided direct evidence for the domain switching near a crack tip subjected to the electric field concentration. The PLZT ceramic samples were mechanically cut and grounded into specimens with the size of 3.5mm×5mm×25mm. XRD revealed an aspect ratio c/a of 1.013, and a spontaneous domain switching strain of 1.3% . The samples were poled under an electric field of 2300V/mm at 120^{o}C, resulting in the ferroelectric domains to align with a polarization normal to the plane. After poling, indentation is performed, followed by the application of the lateral electric field of $0.6E_c$ (E_c＝1100V/mm) to cause the field concentration near the indenting crack. Fig. 1 provided a SEM image near an indentation crack tip [2]. The

actual crack enters the view from the upper-left, and runs down at about $45°$ degrees. Lamellar 90^o domain structure appeared as the black and write strips shown in Fig. 1.

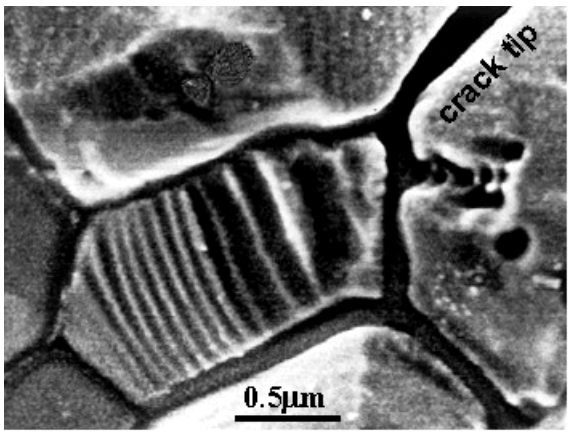

Fig. 1 SEM shows 90^o domain switching bands near a crack tip.

3. Energetics of Domain Bands

The equilibrium domain assemblies is quantified by the free energy minimization. Consider a ferroelectric grain of volume D^3 embedded within a homogenized ferroelectric matrix. Remote stress $\overline{\sigma}_{ij}$ and electric field $\overline{E}_i$ are applied. The formation of domain band structure in the ferroelectric grain causes the following change in system free energy:

$$\Delta U = \Delta U_{\text{Elastic}} + \Delta U_{\text{Electric}} + \Delta U_{\text{Wall}} - \Delta U_{\text{M}}^{\infty} - \Delta U_{\text{E}}^{\infty}, \tag{1}$$

where $\Delta U_{\text{Elastic}}$ denotes the elastic mismatch energy, $\Delta U_{\text{Electric}}$ the electric depolarization energy, ΔU_{Wall} the domain wall energy, and $\Delta U_{\text{M}}^{\infty}$ and $\Delta U_{\text{E}}^{\infty}$ correspond to the works done by the remote stress and electric fields. Denote the spacing of two adjacent domain plates as 2*t*. For the case of an instantaneous $90°$ domain switch, the depolarization energy can be computed as

$$\Delta U_{\text{Electric}} = \frac{2P_s^{\,2}t}{\pi^3 \varepsilon D} f(V_{90}),; \quad f(V_{90}) = \sum_{k=1}^{\infty} \frac{\sin^2(V_{90}k\pi)}{k^3}, \tag{2}$$

where ε denotes the mean square root average of the dielectric constants, P_s the spontaneous polarization, and V_{90} the volume fraction of the switched domain. The domain wall energy has a form of $\Delta U_{\text{Wall}} = \Gamma_{90}/t$, where the 90° domain wall energy Γ_{90} is composed of the coherent domain wall energy Γ_{coh} and the energy Γ_{misfit} of misfit dislocations along the domain wall. The quantity Γ_{coh} assumes a value of $\Gamma_{\text{coh}} = 0.002\text{J/m}^2$ for PZT. The switching released works are

given by $\Delta U_{\mathrm{M}}^{\infty} = V_{90}\overline{\sigma}_{ij}\Delta\gamma_{ij}$ and $\Delta U_{\mathrm{E}}^{\infty} = V_{90}\overline{E}_i\Delta P_i$.

4. Banded Eshelby Inclusion

Consider an infinite region with a banded Eshelby inclusion. The self-equilibrium feature of the residual mismatch stress renders the decomposition of the elastic mismatch energy as $\Delta U_{\mathrm{Elastic}} = \Delta U_{\mathrm{LR}} + \Delta U_{\mathrm{SR}}$. The first term signifies the long-range elastic mismatch energy for a uniform transform in the inclusion. Dimensional consideration dictates that $\Delta U_{\mathrm{LR}} = \alpha(\nu)Y\left(V_{90}\dfrac{c-a}{a}\right)^2$. The transformation strain solution of Eshelby [3] leads to the dimensionless quantity $\alpha(\nu)$ as $(7-5\nu)/[15(1-\nu^2)]$ for a spherical shape, and the value of $3/[16(1-\nu^2)]$ for a cylindrical grain unconstrained in axial direction. The short-range mismatch energy due to the fluctuating mismatch $\tilde{u}_i^*$ along the grain boundary can be computed as

$$\Delta U_{\mathrm{SR}} = -\frac{1}{2D^3}\int_{\partial\Omega}\tilde{t}_i\tilde{u}_i^*\,\mathrm{d}S\,. \tag{3}$$

The misfit dislocations are used to release the long range strain mismatch within the inclusion caused by misfit strains. The domain misfit energy can be obtained as

$$\Gamma_{\mathrm{misfit}} = \frac{Yl}{8\pi(1-\nu^2)}\left(\frac{c-a}{a}\right)^2\left[\ln\frac{l}{4\pi r_0} - \frac{1}{4(1-\nu)}\right]\frac{\sin^2\phi(1+3\cos^2\phi)}{(1+\cos^2\phi)^2}\,. \tag{4}$$

where ϕ denotes the top view angle of domain wall. That angle is measured by microscopy of etched specimen as $70°$.

5. Band Parameters near a Crack Tip

The mismatch along the grain boundary can be expanded by sinusoidal Fourier series, the calculation yields

$$\Delta U_{\mathrm{SR}} = \frac{4(1-\nu)Yf(V_{90})}{(1+\nu)(3-4\nu)\pi^3}\frac{(c-a)^2}{a^2}\frac{t}{D}\frac{1+2\cos^2\phi+5\cos^4\phi}{(1+\cos^2\phi)^2}\,. \tag{5}$$

That leads to a band thickness of

$$t = \sqrt{\frac{\pi^3\Gamma_{90}D}{2f(V_{90})\left[\dfrac{P_s^{\,2}}{\varepsilon} + \dfrac{2(1-\nu)Y}{(1+\nu)(3-4\nu)}\dfrac{(c-a)^2}{a^2}\dfrac{1+2\cos^2\phi+5\cos^4\phi}{(1+\cos^2\phi)^2}\right]}}\,. \tag{6}$$

Substituting the above derivations into (1), one finds the change in system energy as

$$\Delta U = \frac{Y(7-5\nu)}{15(1-\nu^2)}\left(V_{90}\frac{c-a}{a}\right)^2 - V_{90}\left[\frac{c-a}{a}\left(\overline{\sigma}_{22}-\overline{\sigma}_{33}\right)+P_{\mathrm{s}}\left(\overline{E}_2-\overline{E}_3\right)\right] + \frac{2}{\pi}\sqrt{\frac{2f(V_{90})\Gamma_{90}}{\pi D}\left[\frac{P_s^{\,2}}{\varepsilon}+\frac{2(1-\nu)Y}{(1+\nu)(3-4\nu)}\frac{(c-a)^2}{a^2}\frac{1+2\cos^2\phi+5\cos^4\phi}{(1+\cos^2\phi)^2}\right]}. \tag{7}$$

Numerical calculations indicate that the last term only offers an effect of about a few percent in determining the switched volume fraction V_{90}. If that term is neglected, the following explicit expression is derived for V_{90}:

$$V_{90} = \frac{1}{2Y\alpha(\nu)}\frac{a}{c-a}\left[\overline{\sigma}_{22}-\overline{\sigma}_{33}+\frac{a}{c-a}\left(\overline{E}_2-\overline{E}_3\right)P_{\mathrm{s}}\right]. \tag{8}$$

Fig. 1 indicates that the switched ferroelectric grain ahead of the crack has a shape of $1\times1.5\mu$m rectangle, and the length D along the crack extension line is approximately 1.5μm, while the theoretical solution for the domain switching zone is a circle of diameter 1.35μm ahead of the crack but touching the crack tip. The applied field for this case can be evaluated as $2\sqrt{5}E_{\mathrm{app}}$, with $E_{\mathrm{app}} = 0.6E_{\mathrm{c}} = 660$V/mm. Substituting $\overline{E}_2 \approx 2\sqrt{5}E_{\mathrm{app}}$ and $\overline{E}_3 = 0$ into (8), one finds that the volume fraction for switched bands is $\frac{\sqrt{5}}{Y\alpha(\nu)}\left(\frac{a}{c-a}\right)^2 P_{\mathrm{s}}E_{\mathrm{app}}$. For the "soft" ferroelectric ceramics used in this test, the relevant physical constants are $Y = 33$GPa, $\nu = 1/3$, $c/a = 1.013$, $E_{\mathrm{c}} = 1.1\times10^6$ V/m and $P_{\mathrm{s}} = 0.3787$C/m^2. The calculation gives $V_{90} = 0.249$ for fully constrained spherical grain, and $V_{90} = 0.474$ for cylindrical grain unconstrained in the x_3-direction. The measured volume fraction of domain switch is $V_{90} \approx 0.35$. The misfit energy is obtained for the particular domain wall in Fig. 1 as $\Gamma_{\mathrm{misfit}} \approx 0.021$J/m^2. Consequently, Γ_{90} is about 0.023J/m^2. For at a volume fraction of $V_{90} \approx 0.35$, it is found that $f(0.35) \approx 0.902$ from (2). The substitution of the above data, plus $P_{\mathrm{s}} = 0.3787$C/m^2 and $\varepsilon = 1800\varepsilon_0 = 1.593\times10^{-8}$F/m, into (6) gives a predicted domain wall spacing of $t = 0.2178\mu$m. That value is of the same order, but somewhat larger, than the experiment measurement from Fig. 1.

6. Bands near an Indentation Crack of Poled Single Crystals

Two poling modes are taken prior to Vickers indentation. One is the anti-plane poling whose poling field is normal to the observation plane and directed outward; the other is the vertical poling whose poling field lying in the observation plane and directing upward. For the former case, the effect of poling on the observation plane is isotropic, while anisotropic effect can be observed for the latter case.

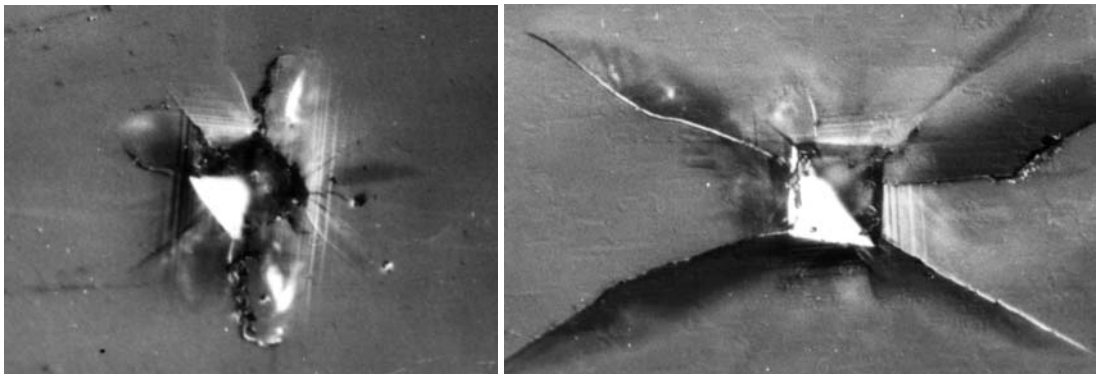

Figure 2 Vickers indents for single crystal barium titanate

Yang *et al*. [4] reported the micrographs of Vickers indents on single crystal barium titanate. Figure 2 shows the micrograph referring to the case of anti-plane poling. Indentation cracks emanated equally from the indenting pyramid in four directions. Domain bands perpendicular to the indenting cracks were formed. Extensions of the indenting cracks trigger the formation of domain bands along their wakes. Since the domain bands are normal to the crack, their switching strains are normal to the indenting crack. Switching strains of this type induce closure and effectively suppress the crack extension. The indentation cracks arrested after small amount of extension.

The right graph of Figure 2 illustrates the microscopy for the case of vertical poling. The cracks extended from the indent pyramid in anisotropic manner. Since the poling is upward, the cracking along the horizontal direction causes less $90°$ domain switching than the cracking along the vertical direction. Accordingly, the domain switch suppresses the crack growth towards a horizontal direction less than that does the crack growth towards a vertical direction. The cracking tilted to the vertical direction was shorter but triggered a wider switching wake, while the cracking tilted to the horizontal direction was longer but triggered a narrower switching wake. Consequently, the fracture toughness of a ferroelectric single crystal after vertical poling is anisotropic: the value against cracking in horizontal direction is lower than that in vertical direction. An interesting phenomenon happened: the strain mismatch along the phase boundary of horizontal bands and vertical bands induced cracks. Since the horizontal domain bands were wider than the vertical bands, the phase boundary of strain mismatch was tilted toward the

horizontal direction. The influence of habit plane of previously formed domain bands dictated that the subsequent formation of domain bands could only be the same horizontal and vertical family, with the same domain boundary mismatch to drive the crack extension along the phase boundary of different domain bands. Subsequently formed domain bands hardly suppressed the propagation of the tilted cracks but drove them. Those cracks tilted in the horizontal direction gradually became the dominant cracks and enjoyed long extension.

Acknowledgement: The present work is sponsored by the National Natural Science Foundation of China.

References

1. Winzer, S.R., Shankar, N. and Ritter, A.P., Designing cofired multilayer electrostrictive actuators for reliability, *J. Am. Ceramic Soc.* **72**(1989), 2246-2257.
2. Fang, F., Yang, W. and Zhu, T., Crack tip 90^0 switching in tetragonal lanthanum-modified lead zirconia titanate under an electric field. *Journal of Materials Research*, **14** (1999), 2940-2944.
3. Eshelby, J.D., Determination of the elastic field of an ellipsoidal inclusion and related problems. Proc. Roy. Society London Ser. **A241**(1957), 376-396.
4. Yang W, Fang F, Tao M. Critical role of domain switching on the fracture toughness of poled ferroelectrics. Int. J. Solids & Structs., 38(2001):2203~2211.